TRANSLATIONAL SCIENCE

METTL3-mediated m^{6}A modification of ATG7 regulates autophagy-GATA4 axis to promote cellular senescence and osteoarthritis progression

Xiang Chen,[1,2] Wang Gong,[1,2] Xiaoyan Shao,[1,2] Tianshu Shi,[1,2] Lei Zhang,[1,2] Jian Dong,[1,2] Yong Shi,[1,2] Siyu Shen,[1,2] Jianghui Qin,[1,2,3] Qing Jiang ![ORCID],[1,2,3] Baosheng Guo ![ORCID] [1,2,3]

[1]State Key Laboratory of Pharmaceutical Biotechnology, Division of Sports Medicine and Adult Reconstructive Surgery, Department of Orthopedic Surgery, Nanjing Drum Tower Hospital, The Affiliated Hospital of Nanjing University Medical School, Nanjing, Jiangsu, China
[2]Jiangsu Key Laboratory of Molecular Medicine, Medical School, Nanjing University, Nanjing, Jiangsu, China
[3]Branch of National Clinical Research Center for Orthopedics, Sports Medicine and Rehabilitation, Nanjing, Jiangsu, China

Correspondence to
Professor Baosheng Guo and Professor Qing Jiang, Division of Sports Medicine and Adult Reconstructive Surgery, Nanjing University Medical School Affiliated Nanjing Drum Tower Hospital, Nanjing, Jiangsu, China; borisguo@nju.edu.cn, qingj@nju.edu.cn

![Check for updates]

ABSTRACT

Objective The aim of the study was to investigate the role and regulatory mechanisms of fibroblast-like synoviocytes (FLSs) and their senescence in the progression of osteoarthritis (OA).

Methods Synovial tissues from normal patients and patients with OA were collected. Synovium FLS senescence was analysed by immunofluorescence and western blotting. The role of methyltransferase-like 3 (METTL3) in autophagy regulation was explored using N6-methyladenosine (m^{6}A)-methylated RNA and RNA immunoprecipitation assays. Mice subjected to destabilisation of the medial meniscus (DMM) surgery were intra-articularly injected with or without pAAV9 loaded with small interfering RNA (siRNA) targeting METTL3. Histological analysis was performed to determine cartilage damage.

Results Senescent FLSs were markedly increased with the progression of OA in patients and mouse models. We determined that impaired autophagy occurred in OA-FLS, resulting in the upregulation of senescence-associated secretory phenotype (SASP). Re-establishment of autophagy reversed the senescent phenotype by suppressing GATA4. Further, we observed for the first time that excessive m^{6}A modification negatively regulated autophagy in OA-FLS. Mechanistically, METTL3-mediated m^{6}A modification decreased the expression of autophagy-related 7, an E-1 enzyme crucial for the formation of autophagosomes, by attenuating its RNA stability. Silencing METTL3 enhanced autophagic flux and inhibited SASP expression in OA-FLS. Intra-articular injection of synovium-targeted METTL3 siRNA suppressed cellular senescence propagation in joints and ameliorated DMM-induced cartilage destruction.

Conclusions Our study revealed the important role of FLS senescence in OA progression. Targeted METTL3 inhibition could alleviate the senescence of FLS and limit OA development in experimental animal models, providing a potential strategy for OA therapy.

INTRODUCTION

Osteoarthritis (OA), the most prevalent joint disease in late life, is primarily characterised by progressive loss of cartilage matrix, accompanied by pathological changes in other joint components, including subchondral bone sclerosis and synovial inflammation.[1] Incident symptomatic knee OA has been reported to peak between 55 and 64 years of age.

Key messages

What is already known about this subject?
► The chronic presence of senescent cells is closely associated with the development of osteoarthritis (OA). However, the underlying mechanisms remain unclear.

What does this study add?
► Senescent fibroblast-like synoviocytes (FLSs) affect the normal function of chondrocytes in vitro and in vivo.
► We demonstrated the critical role of methyltransferase-like 3 (METTL3)/YTH N6-methyladenosine RNA-binding protein 2-mediated N6-methyladenosine (m^{6}A) modification of the autophagy-related 7 messenger RNA in regulating autophagy and cellular senescence.
► Inhibition of METTL3 effectively suppresses the senescence of FLS and decelerate OA development.

How might this impact on clinical practice or future developments?
► Our study highlights the functional importance of the m^{6}A methylation machinery in autophagy, which provides insights into the underlying molecular mechanisms of METTL3 in regulating cellular senescence and the development of therapeutic strategies for the treatment of OA.

Moreover, the prevalence of OA increased with age, ranging from 13% in non-obese men to 32% in obese women over 85 years of age.[2] With the ageing of the world population, the number of older adults affected by OA and in need of joint replacement will substantially increase in the following decades. In older adults, a variety of factors related to ageing may contribute to the development of OA. Mitochondrial dysfunction, oxidative stress and reduced autophagy alter chondrocyte function, promoting catabolic processes and cell death during anabolic processes.[3] Thus, improving our understanding of how ageing promotes OA progression would provide novel strategies to slow or stop the

development of the disease, which may have a major impact on public health.

The chronic presence of senescent cells is tightly associated with tissue function loss and age-related chronic diseases such as OA. Cellular senescence is an essential hallmark of ageing, and chondrocytes have various features that are characteristic of senescent cells during ageing and OA progression.[3 4] Senescent cells are characterised by inability to divide, resistance to apoptosis and robust secretome of senescence-associated secretory phenotype (SASP), which could alter the structure and function of the surrounding cells and tissues.[5] Increased production of proinflammatory mediators, including interleukin (IL)-1, IL-6 and matrix metalloproteinase (MMP)3, is a feature of SASP that overlaps with mediators that contribute to the development of OA. To date, the molecular mechanisms associated with the regulation of cellular senescence in OA remain elusive.

It has been reported that large numbers of synoviocytes are senescent in the pathogenesis of OA.[6] In our study, we found a dramatic increase in senescent cells in the synovium region 2 weeks after destabilisation of the medial meniscus (DMM) surgery, which preceded the events of chondrocyte senescence and cartilage degradation. Increased secretion of proinflammatory cytokines and MMPs by the synovium is believed to be involved in the degradation of joint cartilage.[7] Growing evidence supports the notion that the provoked SASP expression and accelerated ageing process are tightly correlated with autophagy inhibition.[8] Autophagy activation can effectively suppress the severity of experimental OA.[9] As a normal cellular metabolic process, autophagy mediates the delivery of cellular components to lysosomes and promotes cell survival under stress.[10] The factors implicated in ageing, such as the loss of proteostasis and accumulation of oxidative damage, genomic instability and epigenomic alteration, are modified through autophagy. Enhancing the autophagy process is regarded as a common characteristic of all evolutionarily conserved antiageing interventions.[11] Articular chondrocytes rely on autophagy as the primary mechanism for maintaining normal function and survival.[12 13] During ageing, autophagy gradually decreases in chondrocytes, thus inducing senescence, which ultimately results in aggravated OA severity.[14] However, the mechanisms underlying impaired autophagy in OA progression are not well understood.

Cell growth and survival depend on the fine-tuning regulation of gene expression at both the transcriptional and translational levels.[15] N6-methyladenosine (m6A) is a widespread post-transcriptional modification of RNA that determines messenger RNA (mRNA) stability, splicing, transport, localisation and translation efficiency.[16 17] Increasing pieces of evidence suggest that m6A participates deeply in various cellular processes, including DNA damage, autophagy and cellular senescence.[18–20] The m6A modification is dynamic and reversible, and it can be catalysed by m6A methyltransferases and removed by m6A demethylases.[21 22] In addition, m6A functions through 'reader' proteins, which selectively recognise and directly or indirectly bind to the m6A motif to affect mRNA function. YTH N6-methyladenosine RNA-binding protein (YTHDF), a class of m6A readers, includes YTHDF1 and YTHDF2. YTHDF1 promotes the translation of m6A-modified mRNA, while YTHDF2 suppresses the stability and mediates alternative splicing of m6A-modified-mRNA. Recently, it was reported that methyltransferase-like 3 (METTL3), the core component of the m6A methyltransferase, was significantly elevated in the synovium of human rheumatoid arthritis. METTL3 knockdown effectively suppressed inflammatory and MMP factor expression in fibroblast-like synoviocytes (FLSs).[23] In addition, inhibition of METTL3 significantly reduced the IL-1β-induced degeneration of chondrocytes.[24] However, the biological significance of m6A modification and the potential regulatory mechanisms of cellular senescence in FLS remain incompletely understood.

In this study, we demonstrated for the first time the critical role of senescent FLS in OA progression in vitro and in vivo and found a positive correlation between m6A modification and FLS senescence. Further studies revealed that METTL3 influenced autophagy activity by affecting the stability of autophagy-related 7 (ATG7) mRNA in an m6A-YTHDF2 dependent manner, which subsequently promoted FLS senescence and OA progression. Conversely, METTL3 suppression in FLS effectively inhibited the senescence of FLS and attenuated OA progression in the DMM-induced OA mouse model. Thus, our work implicates METTL3 as a potential therapeutic target for OA treatment.

MATERIALS AND METHODS
Detailed experimental procedures are described in the online supplemental materials and methods (see online supplemental file 1).

RESULTS
FLS senescence and impaired autophagy are closely associated with the progression of OA
To explore the role of cellular senescence in OA development, we first examined the expression of p16^{INK4a} and p21, a typical biomarker of senescent cells, in human OA synovial tissues. The protein and mRNA levels of p16^{INK4a} and p21 were dramatically elevated in the synovium of patients with OA (figure 1A–D). We further observed the accumulation and phenotypical characterisation of senescent FLSs in OA synovial tissues, as confirmed by double-positive immunostaining for p16^{INK4a} and vimentin, a marker of FLS (figure 1E). In addition, the primary FLSs isolated from the synovium of patients with OA also exhibited various senescent phenotypes, including increased expression levels of senescence-associated β-galactosidase (SA-β-Gal), p16^{INK4a} and p21, and enhanced secretion of IL-1β (online supplemental figure S1A–D and S2A). Interestingly, we found decreased accumulation of autophagic vesicles by transmission electron microscopy analyses in the synovium of patients with OA, indicating deficient autophagy in the OA synovium (figure 1F). In addition, we further measured the autophagic markers LC3B-II (a typical marker of autophagosomes) and p62 (a protein regulating autophagic clearance of dysfunctional organelles or aggregates) in the synovium and found lower expression of LC3B-II and higher levels of p62 in the synovium of patients with OA, compared with patients without OA (figure 1C).

To further verify the aforementioned findings and explore FLS senescence during OA development, we established a post-traumatic OA model by DMM and analysed the number of senescent FLSs identified by the positive expression of p16^{INK4a} during OA development. Compared with sham-operated mice, we found that the number of p16^{INK4a}-positive FLSs in the synovium of DMM mice significantly increased in a time-dependent manner (figure 1G and online supplemental figure S1E). In addition, we found a large number of p16^{INK4a}-expressing cells in the synovium region 2 weeks after surgery, which occurred earlier than chondrocyte senescence (online supplemental figure S3). Meanwhile, the cartilage degradation and the Osteoarthritis Research Society International (OARSI) score were significantly aggravated with time during the course of DMM-induced OA pathogenesis (figure 1H), which was tightly correlated with enhanced FLS senescence (figure 1I). In
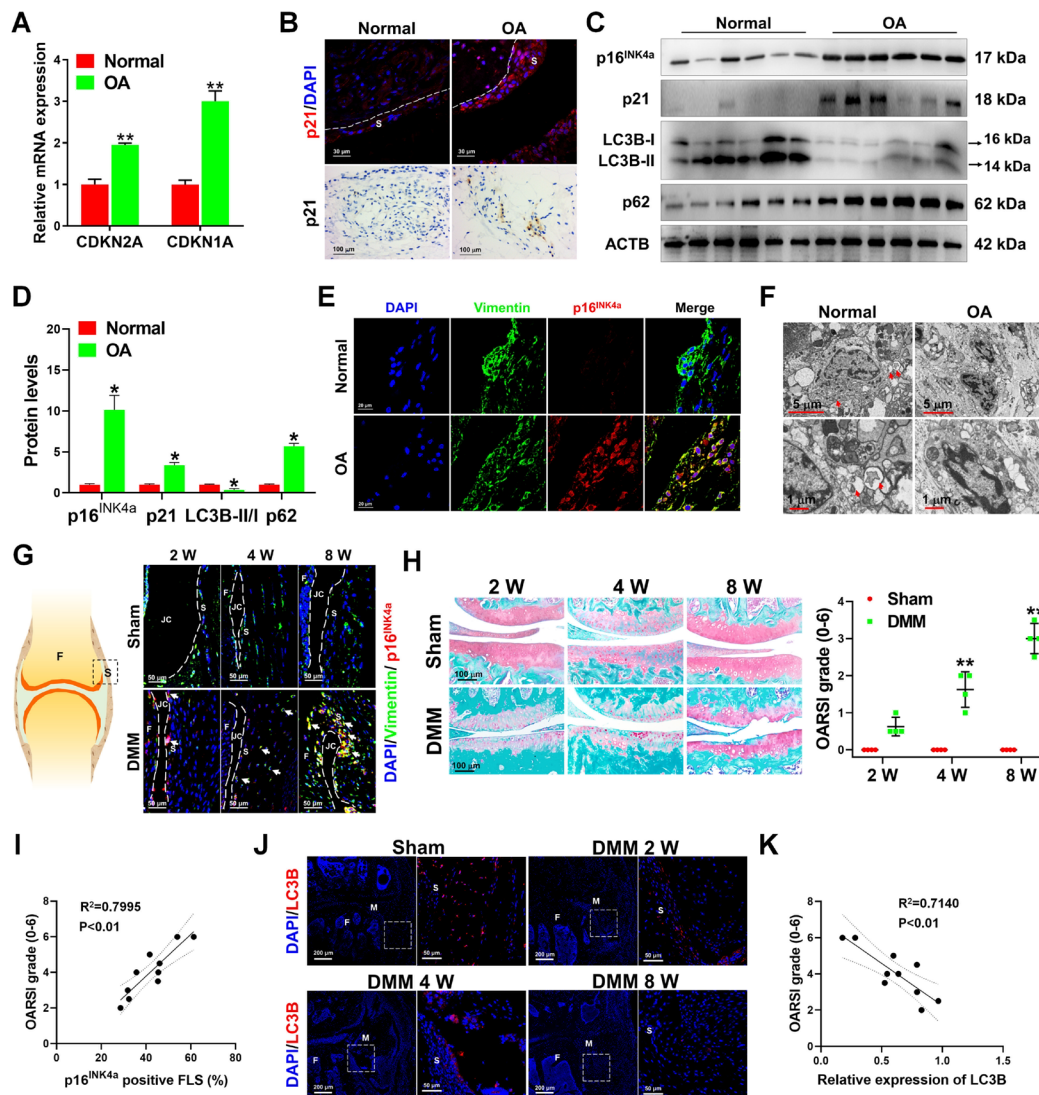
Figure 1 FLS senescence and impaired autophagy closely associates with the progression of OA. (A) Quantitativ PCR analysis of messenger RNA levels for CDKN2A and CDKN1A in synovial tissues from patients with OA (OA) and patients without OA (normal). n=10 per group. **P<0.01. (B) Representative images of immunostaining for p21 in synovial tissues from patients with OA (OA) and patients without OA (normal). (C) Western blot analysis of p16^{INK4a}, p21, LC3B and p62 in synovial tissues from patients with OA (OA) and patients without OA (normal). (D) Protein quantification of (C) via ImageJ. n=6 per group. *P<0.05. (E) Representative images of coimmunostaining of vimentin and p16^{INK4a} in synovial tissues from patients with OA (OA) and patients without OA (normal). (F) The representative electron microscopy images of human normal and OA synovium. Red arrowheads indicate autophagic vesicles. (G) The representative images of coimmunostaining of vimentin and p16^{INK4a} in the synovium from control mice (sham) or post-traumatic mice at 2, 4 and 8 weeks after DMM surgery. The dotted box indicates the amplified synovium regions. Arrowheads indicate double-positive cells. (H) The representative safranin O staining images of osteoarthritic knee joints from control mice (sham) or post-traumatic mice at 2, 4 and 8 weeks after DMM surgery. The severity of OA-like phenotype was analysed by grading histological sections in medial femoral condyles and the medial tibial plateau using the OARSI score system. n=4 of each group. **P<0.01. (I) Correlation curves between OARSI grade and the number of p16^{INK4a}-positive FLS in the synovium of mice suffered with DMM. (J) The representative images of immunofluorescence of LC3B in synovium of control mice (sham) or post-traumatic mice at 2, 4 and 8 weeks after DMM surgery. The dotted box indicates the amplified synovium regions. (K) Correlation curves between OARSI grade and LC3B expression in the synovium of mice that suffered from DMM surgery. All data were presented as the means±SEM. Paired t-test (A,D) and repeated-measures two-way analysis of variance (H) were used for statistical analysis. ACTB, β-actin; DAPI, 4',6-diamidino-2-phenylindole; DMM, destabilisation of the medial meniscus; F, femur; FLS, fibroblast-like synoviocyte; JC, joint cavity; M, meniscus; S, synovium; OA, osteoarthritis; OARSI, Osteoarthritis Research Society International.

addition, we also demonstrated that the expression of LC3B was dramatically decreased during the progression of DMM-induced OA (figure 1J), which was negatively correlated with OARSI scores (figure 1K). These results indicate that FLS senescence and impaired autophagy are tightly correlated with OA progression.

Senescent FLSs contributed to the catabolic effects of chondrocytes in vivo and in vitro

To further verify whether senescent FLS could accelerate the pathological progression of OA, we cocultured human chondrocytes (C28/I2 cells) with either primary FLSs from patients with OA (OA-FLS) or FLSs from patients without OA (Con-FLS,
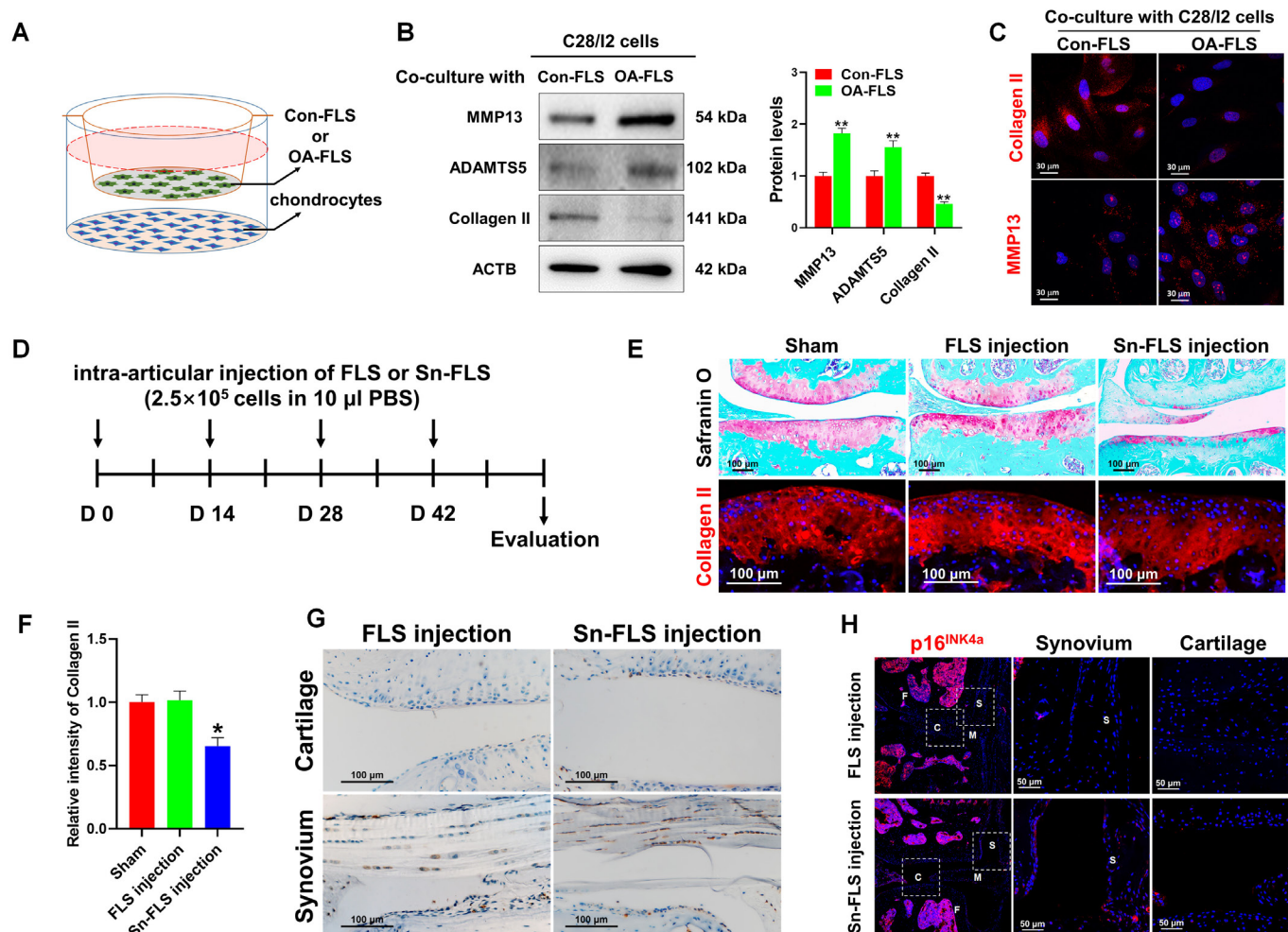
Figure 2 Senescent FLS promotes cartilage degradation in vitro and in vivo. (A) Experimental design diagram of coculture human Con-FLS or OA-FLS with chondrocytes free of direct contact. (B) Western blot analysis for the protein expression of MMP13, ADAMTS5 and collagen II in human chondrocytes (C28/I2 cells) after coculture with human Con-FLS or OA-FLS (passage 2) for 48 hours. n=3. *P<0.05. (C) Immunofluorescence staining of collagen II and MMP13 in C28/I2 cells after coculture with human Con-FLS or OA-FLS for 48 hours. (D) Experimental design diagram of intra-articular injection of normal FLS (FLS) or Sn-FLS induced by bleomycin on mice. (E) The representative images of safranin O staining (top panel) and collagen II staining (bottom panel) for joint from mice after intra-articular injection of FLS or Sn-FLS. (F) Quantification of collagen II expression in cartilage via ImageJ. n=3 per group. *P<0.05. (G,H) The representative images of immunohistochemistry (G) and immunofluorescence (H) staining of p16[INK4a] in cartilage and synovium from mice after intra-articular injection of FLS or Sn-FLS. All data were presented as the means±SEM. Paired t-test (B) and one-way analysis of variance with Dunnett's multiple comparisons test (F) were used for statistical analysis. C, cartilage; F, femur; FLS, fibroblast-like synoviocyte; M, meniscus; MMP, matrix metalloproteinase; OA, osteoarthritis; S, synovium; Sn-FLS, senescent fibroblast-like synoviocyte.

figure 2A). Interestingly, we detected increased expression of MMP13 and ADAMTS5 and decreased expression of collagen II in C28/I2 cells after coculture with OA-FLS (figure 2B,C). In addition, to further investigate the effects of senescent FLSs on cartilage degradation in vivo, we used bleomycin, a DNA-damaging chemical agent, to induce robust cellular senescence in mouse FLSs, as indexed by the induction of SA-β-Gal activity (online supplemental figure S4A). The excessive FLS senescence induced by bleomycin was further confirmed by increased expression of p16[INK4a] and p21 and elevated mRNA levels of SASP (online supplemental figure S4B,C). Then, mice without DMM surgery were intra-articularly injected with either 2.5×10^5 normal FLSs or senescent FLSs induced by bleomycin treatment (figure 2D). At day 56 after the first injection, we found decreased safranin O staining and lower expression of collagen II in mice injected with senescent FLSs compared with mice injected with normal FLSs (figure 2E,F), accompanied by elevated expression of p16[INK4a] in the synovium and cartilage

(figure 2G,H). This indicated that exogenous injection of senescent FLS could trigger cartilage dysfunction and induce senescence of the synovium and cartilage.

Autophagy was impaired in senescent FLSs from patients with OA and in DMM-induced OA mice

Recently, impaired autophagy has been implicated in the ageing of various model organisms, possibly contributing to enhanced cellular senescence,[25 26] both in patients with OA and in OA mice models. We observed reduced LC3B expression and elevated levels of p62 in FLSs in both patients with OA and DMM mouse models (figure 3A,B, and online supplemental figure S5A,B). In addition, we found that LC3B was significantly decreased and p62 was dramatically elevated in p16[INK4a] positive cells in both patients with OA and DMM-induced OA models (figure 3C,D, and online supplemental figure S5C,D). To further confirm whether the reduced autophagic structures in OA-FLS were
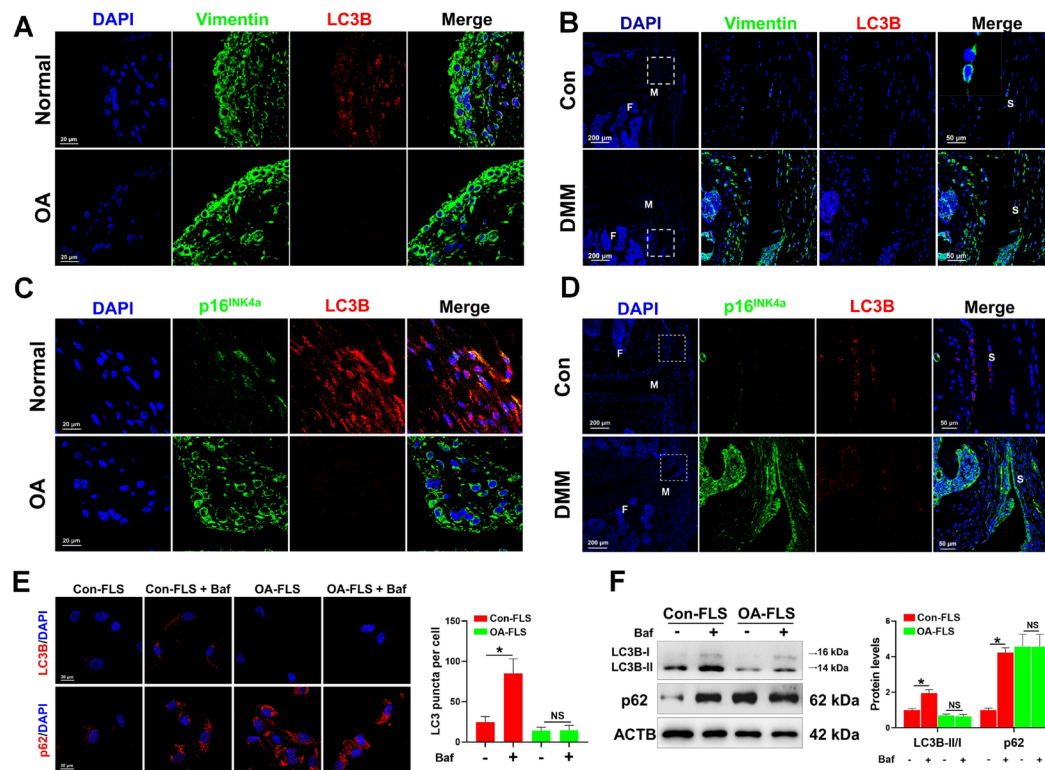
Figure 3 Autophagy is impaired in FLS from patients with OA and DMM-induced OA mice. (A, B) The representative images of double fluorescent immunostaining for vimentin with LC3B in the synovium from patients with OA (A) and post-traumatic mice (B) 8 weeks after DMM surgery. The dotted box indicates the amplified synovium regions. (C, D) The representative images of double fluorescent immunostaining for p16[INK4a] and LC3B in the synovium from patients with OA (C) and post-traumatic mice (D) 8 weeks after DMM surgery. The dotted box indicates the amplified synovium regions. (E) The representative images of immunofluorescent labelling of LC3B and p62 in human Con-FLS or OA-FLS (passage 2) with the treatment of bafilomycin A1 (Baf, 50 nM) or not; the average number of LC3B puncta per cell was quantified via ImageJ (right panel). n=3. *P<0.05. (F) Western blot analysis of LC3B and p62 in human Con-FLS or OA-FLS (passage 2) with the treatment of Baf or not. n=3. *P<0.05. All data are presented as the mean±SEM. One-way analysis of variance with Dunnett's multiple comparisons was used for statistical analysis. DMM, destabilisation of the medial meniscus; F, femur; FLS, fibroblast-like synoviocyte; M, meniscus; NS, not significant; OA, osteoarthritis; S, synovium.

caused by autophagy impairment or by enhanced autophagic degradation, we used the autophagy-flux inhibitor bafilomycin, which could increase LC3B by preventing lysosomal degradation.[27] Bafilomycin treatment increased the number of LC3B puncta and elevated the levels of p62 in Con-FLS. However, treatment with bafilomycin did not increase LC3B and p62 expression in OA-FLS (figure 3E,F), indicating that OA-FLS lacks the capacity for further autophagosome formation and that the degradation capacity of lysosomes was already at a low level in OA-FLS.

Impaired autophagy in FLS accelerated cellular senescence in a GATA4-dependent manner

To assess whether autophagy mediated FLS senescence, we performed additional autophagy activation and blockade experiments. On one hand, activation of autophagy by rapamycin effectively increased the protein levels of LC3B-II and LC3 puncta per cell (figure 4A and online supplemental figure S6) and suppressed a series of events including p16[INK4a], p21 and p62 expressions, as well as IL-1β secretion in OA-FLS (figure 4A and online supplemental figure S2B). On the other hand, inhibition of autophagy via 3-methyladenine (3-MA) significantly decreased LC3B-II levels, accompanied by elevated expression of p62, p16[INK4a] and p21 in Con-FLS (figure 4B). Furthermore, we found that GATA4, a recently described senescence regulator,[8] was significantly increased in OA-FLS both in vivo

and in vitro (figure 4C,D, and online supplemental figure S7). GATA4 knockdown significantly suppressed the secretion of IL-1β (online supplemental figure S2C). In addition, recovery of autophagy via rapamycin in OA-FLS could effectively decrease the expression of GATA4, whereas 3-MA treatment significantly promoted the protein level of GATA4 in Con-FLS (figure 4A,B). To further investigate whether autophagy prevented cellular senescence by suppressing GATA4, Con-FLSs were transfected with pcDNA3.1-GATA4 or GATA4 small interfering RNA (siRNA) with or without rapamycin or 3-MA treatment. GATA4 knockdown alleviated the 3-MA-induced expression of p16[INK4a], p21 and SASP (figure 4E,F). In contrast, upregulation of GATA4 could contribute to the expression of p16[INK4a], p21 and SASP (figure 4G,H).

Elevated m⁶A levels correlated with impaired autophagy in OA-FLS

Recently, an increasing number of studies have reported that m⁶A modification controls autophagy activity in various physiological processes, including tumorigenesis and cell apoptosis.[18 28] To determine whether m⁶A modification was involved in regulating autophagy activity in FLS during the development of OA, the levels of m⁶A were measured by using immunofluorescence. We observed that m⁶A expression was significantly increased in both the FLSs of patients with OA and DMM mouse models (figure 5A–C and online
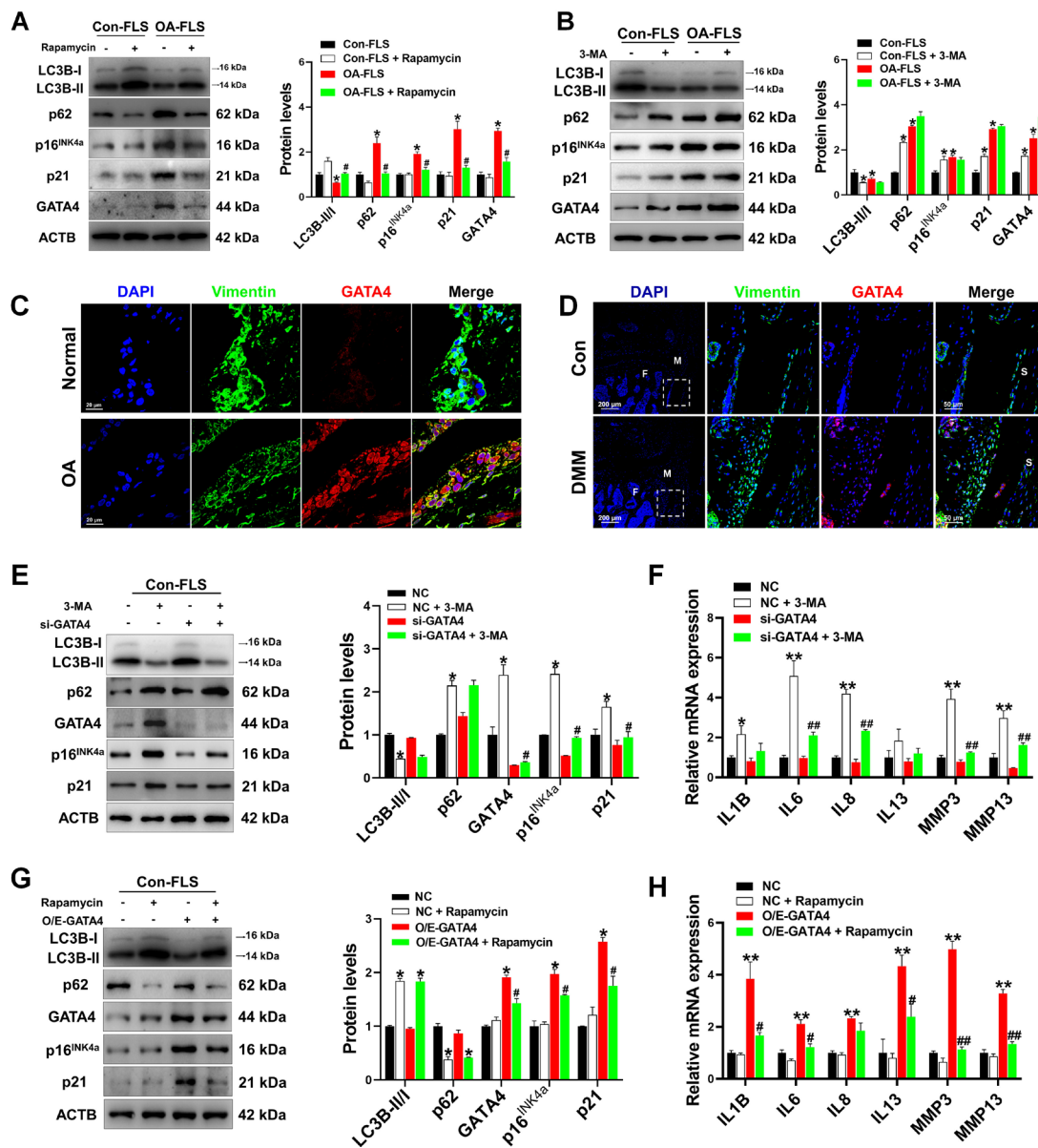
Figure 4 Autophagy regulates cellular senescence in a GATA4-dependent manner. (A) Western blot analysis of the protein levels for autophagy markers (LC3B and p62), cellular senescence markers (p16[INK4a] and p21) and GATA4 in human Con-FLS and OA-FLS (passage 2) treated with or without rapamycin (50 nM) for 48 hours. n=3 per group. *P<0.05 vs Con-FLS; #P<0.05 vs OA-FLS. (B) Western blot and analysis of the protein levels for autophagy markers (LC3B and p62), cellular senescence markers (p16[INK4a] and p21) and GATA4 in human Con-FLS and OA-FLS (passage 2) treated with or without 3-MA (1 mM) for 48 hours. n=3 per group. *P<0.05 vs Con-FLS. (C,D) The representative images of double immunofluorescent staining for vimentin and GATA4 in human synovium (C) and post-traumatic mice 8 weeks after DMM surgery (D). The dotted box indicates the amplified synovium regions. (E) Western blot analysis of protein levels for autophagy markers (LC3B and p62), cellular senescence markers (p16[INK4a] and p21) and GATA4 in human Con-FLS (passage 2) transfected with siRNA targeting GATA4 (si-GATA4) followed by 3-MA treatment for 48 hours. n=3 per group. *P<0.05 vs NC; #P<0.05 vs NC +3-MA. (F) qPCR analysis of SASP-related inflammatory cytokines (IL-1β, IL-6, IL-8 and IL-13), MMP3 and MMP13 in indicated groups. n=3 per group. *P<0.05, **P<0.01 vs NC; ##P<0.01 vs NC +3-MA. (G) Western blot analysis of protein levels for autophagy markers (LC3B and p62), cellular senescence markers (p16[INK4a] and p21) and GATA4 in human Con-FLS (passage 2) transfected with pcDNA3.1-GATA4 (O/E-GATA4) vector followed by the treatment of rapamycin for 48 hours. n=3 per group. *P<0.05 vs NC; #P<0.05 vs O/E-GATA4. (H) qPCR analysis of SASP-related inflammatory cytokines (IL-1β, IL-6, IL-8 and IL-13), MMP3 and MMP13 in indicated groups. n=3 per group. **P<0.01 vs NC; #P<0.05, ##P<0.01 vs O/E-GATA4. All data were presented as the means±SEM. One-way analysis of variance with Dunnett's multiple comparisons was used for statistical analysis. 3-MA, 3-methyladenine; DMM, destabilisation of the medial meniscus; F, femur; FLS, fibroblast-like synoviocyte; IL, interleukin; M, meniscus; MMP, matrix metalloproteinase; NC, negative control; OA, osteoarthritis; O/E, overexpression; qPCR, quantitative PCR; S, synovium; SASP, senescence-associated secretory phenotype; siRNA, small interfering RNA.

supplemental figure S9A). Given that m⁶A modification is mainly regulated by the m⁶A methyltransferase complex,[29] we measured the mRNA levels of METTL3, METTL14, WT1-associated protein (WTAP), fat mass and obesity-associated protein (FTO), and AlkB homolog 5 (ALKBH5) in the OA synovium and OA-FLSs. We found that the mRNA expression of METTL3 was significantly upregulated, while the mRNA expression of the other genes did not change significantly
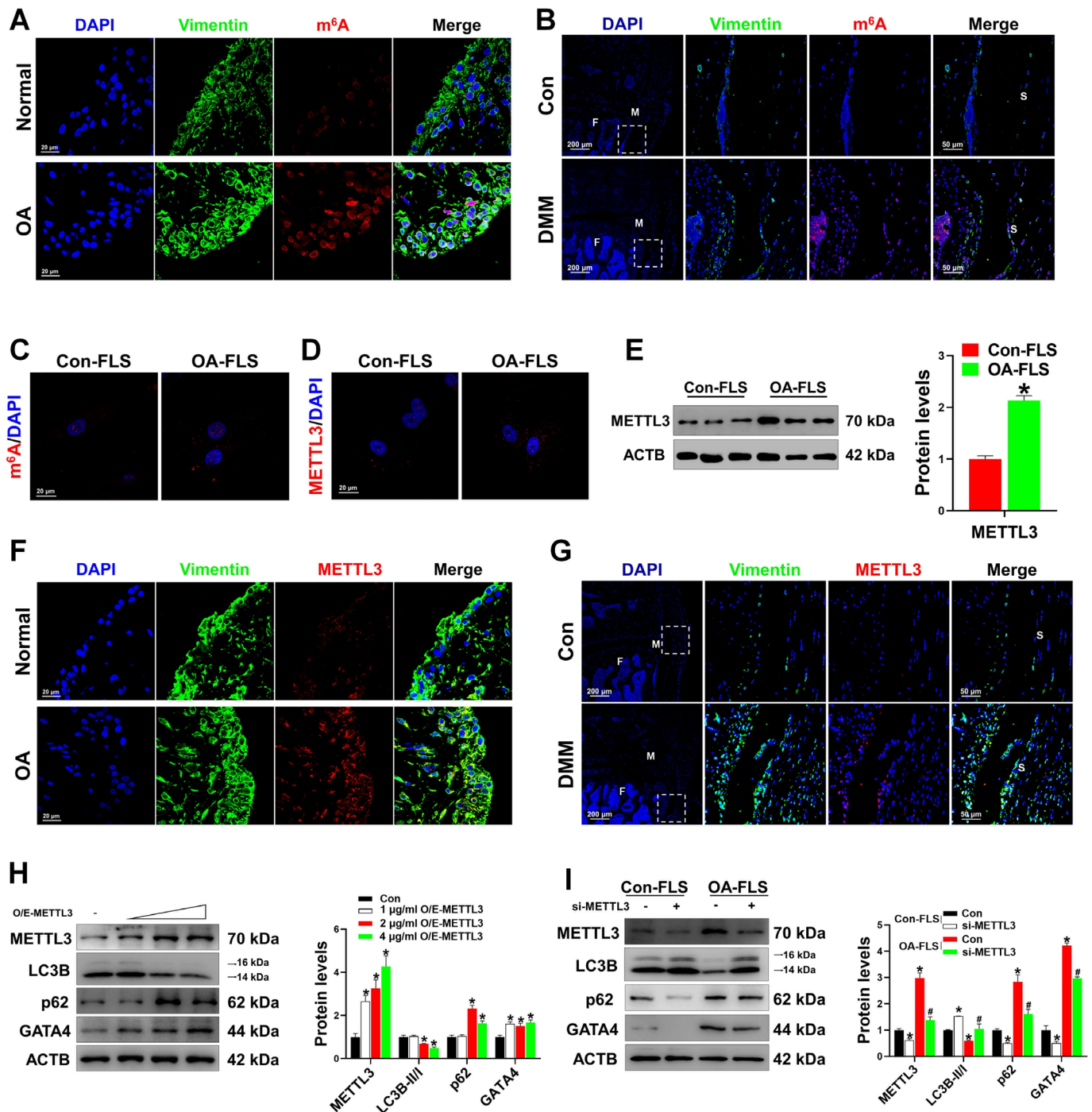
Figure 5 Elevated m^{6}A levels contribute to impaired autophagy in OA-FLS. (A,B) The representative images of double immunofluorescent labelling for vimentin and m^{6}A in synovium from patients with OA (A) and post-traumatic mice 8 weeks after DMM surgery (B). The dotted box indicates the amplified synovium regions. (C) The representative images of immunofluorescent detection for m^{6}A in human Con-FLS and OA-FLS (passage 2). (D) The representative images of immunofluorescent staining of METTL3 in human Con-FLS and OA-FLS (passage 2). (E) Western blot analysis of METTL3 protein levels in human FLS (passage 2) derived from patients with OA or patient without OA. n=3. *P<0.05. (F,G) The representative images of double immunofluorescent labelling of vimentin and METTL3 in synovium from patients with OA (F) and DMM-induced OA mice (G) at 8 weeks after surgery. The dotted box indicates the amplified synovium regions. (H) Western blot analysis of protein levels for METTL3, LC3B, p62 and GATA4 in human Con-FLS (passage 2) after transfection with pcDNA3.1-METTL3 vector (O/E-METTL3, O/E) at different dosages (1, 2 and 4 µg/mL) for 3 days or not. n=3. *P<0.05. (I) Western blot analysis of protein levels for METTL3, LC3B, p62 and GATA4 in human Con-FLS and OA-FLS (passage 2) after transfected with si-METTL3 and cultured for 3 days or not. n=3. *P<0.05 vs Con-FLS; #P<0.05 vs OA-FLS. All data were presented as the means±SEM. Paired t-test (E) and one-way analysis of variance with Dunnett's multiple comparisons (H,I) were used for statistical analysis. 3-MA, 3-methyladenine; DMM, destabilisation of the medial meniscus; F, femur; FLS, fibroblast-like synoviocyte; S, synovium; M, meniscus; m^{6}A, N6-methyladenosine; METTL-3, methyltransferase-like 3; OA, osteoarthritis; O/E, overexpression.

(online supplemental figure S8). Consistent with these findings, the protein levels of METTL3 were also profoundly increased in FLS isolated from the synovium of patients with OA (figure 5D,E). We further confirmed this finding by double labelling of vimentin and METTL3 using immunofluorescence staining in both human OA synovium and DMM-induced OA models (figure 5F,G). To further confirm whether autophagy repression in OA was due to elevated m[6]A modification and METTL3 expression, human FLSs were overexpressed with METTL3. We observed that upregulation of METTL3 elevated m[6]A levels (online supplemental figure S9B,C), accompanied by decreased expression of LC3B-II and enhanced expression of p62 and GATA4 (figure 5H). On the contrary, METTL3 knockdown decreased the levels of m[6]A (online supplemental figure S9B,C), upregulated the expression of LC3B-II, and suppressed the protein levels of p62 and GATA4 in OA-FLS (figure 5I). These results revealed that METTL3-mediated m[6]A modification plays a critical role in autophagy-regulated senescence in FLS.

METTL3-mediated m[6]A modification induced the decay of the ATG7 transcript in a YTHDF2-dependent manner

To investigate the role of m[6]A modification and verify METTL3 as its potential target gene in autophagy, we first employed quantitative PCR (qPCR) analysis to examine the mRNA levels of autophagy-related genes, which tightly execute and control the process of autophagy from initiation to closure.[30] Our results showed that the mRNA levels of ATG7 were significantly attenuated in both the human OA synovium and OA-FLSs (online supplemental figure S10A,B). Consistently, the ATG7 protein levels were markedly decreased in human OA-FLSs and the DMM mouse model (figure 6A,B). Upregulation of METTL3 significantly decreased the expression of ATG7 (online supplemental figure S10C and figure 6C). In contrast, METTL3 knockdown upregulated the expression of ATG7 in OA-FLS (figure 6D).

Given that we found a negative correlation between METTL3 and autophagy, we further confirmed whether METTL3 influenced autophagy by regulating the expression of ATG7. Upregulation of ATG7 effectively alleviated METTL3-induced LC3B-II reduction and decreased the expression of p62 and GATA4 in Con-FLS (figure 6E). Knockdown of ATG7 also suppressed the METTL3 knockdown-induced LC3B-II increase, and enhanced the levels of p62 and GATA4 in Con-FLS (figure 6F), suggesting that METTL3-induced autophagy defects in FLS were mediated through the inhibition of ATG7. Next, we performed sequence analysis of the ATG7 transcript and found three sites of m[6]A modification within the coding sequence region and five m[6]A sites in the 3′-untranslated region (UTR) (figure 6G). The m[6]A RNA-immunoprecipitation (RIP) analyses demonstrated that m[6]A was significantly enriched at sites 1, 2, 4, 5 and 7 (figure 6H). Compared with Con-FLS, m[6]A enrichment at sites 4 and 7 was dramatically increased in OA-FLS (figure 6I), which was markedly decreased on METTL3 knockdown (figure 6J). These results suggest that METTL3 targets the ATG7 transcript and regulates ATG7 in an m[6]A-dependent manner.

While METTL3 serves as a 'writer' for m[6]A on ATG7, potential m[6]A-selective-binding proteins are required to recognise m[6]A-modified mRNA and exert regulatory functions. YTHDF1 has been reported to promote the translation of targeted m[6]A-modified mRNA, while YTHDF2 selectively recognises and destabilises m[6]A-modified mRNA.[31] To further illustrate whether YTHDF1 or YTHDF2 selectively targeted m[6]A-modified mRNA

of ATG7 to regulate its expression in FLS, we transfected FLSs with the METTL3 plasmid, followed by treatment with or without si-YTHDF1 and si-YTHDF2, respectively. We found that knockdown of YTHDF2 markedly alleviated the METTL3-induced reduction of ATG7 protein expression, whereas YTHDF1 knockdown did not affect ATG7 protein expression. This indicated that the m[6]A-modified mRNA of ATG7 by METTL3 was a target of YTHDF2 (figure 6K). In addition, we performed RIP-qPCR analyses to confirm that ATG7 indeed interacted with YTHDF2 but not with YTHDF1 (figure 6L,M). Taken together, our results demonstrate that METTL3 regulates ATG7 expression in a YTHDF2-dependent manner.

METTL3 regulated cellular senescence and SASP expression in vitro

To further explore the functional role of METTL3 in regulating FLS senescence, we overexpressed METTL3 in human FLSs via transfection with the METTL3 plasmid. We demonstrated that upregulation of METTL3 significantly elevated the expression of p16[INK4a] and p21 (figure 7A,B), and the mRNA levels of SASP (figure 7B) in human FLSs. The β-galactosidase assay also confirmed that METTL3 promoted senescence in FLSs (figure 7C). Next, we investigated whether downregulation of METTL3 by transfection with METTL3 siRNA could reverse senescence in OA-FLS. We observed that METTL3 knockdown obviously suppressed p16[INK4a] and p21 expressions (figure 7D,E) and decreased SASP expression and IL-1β secretion (figure 7E and supplemental figure S2C) in OA-FLS. To further confirm the aforementioned findings, mouse FLSs were treated with bleomycin, followed by transfection with or without si-METTL3. We also found that knockdown of METTL3 effectively alleviated bleomycin-induced p16[INK4a], p21 and SASP expressions (figure 7F), as well as β-galactosidase production (figure 7G,H) in mouse FLSs. Together, these data demonstrate that METTL3 plays a critical role in promoting FLS senescence, and METTL3 may act as a potential therapeutic target for impairing cellular senescence in FLSs.

Synovium-targeted inhibition of METTL3 alleviated the progression of OA in a DMM mouse model

A previous study reported that the synovial fibroblast-targeting peptide motif (HAP-1) could effectively deliver drug-encapsulated liposomes to synovial fibroblasts in the inflamed synovium.[32] To confirm whether targeted inhibition of METTL3 in FLS could suppress OA progression, we inserted HAP-1-encoding DNA sequences into the N-terminus of the VP2 domain to construct an FLS-targeted adeno-associated virus vector (rAAV9.HAP-1) (figure 8A). To test whether HAP-1 insertion affects the cellular transfection ability of rAAV9, the vectors were infected with FLS and chondrocyte progenitor cells (ATDC5). Compared with rAAV9, rAAV9.HAP-1 showed a modest increase in transfection efficiency, and low enhanced green fluorescent protein (EGFP) expression was detected in ATDC5 cells (figure 8B). Since the rAAV9.HAP-1 engineered capsid retained full transfection activity in vitro, we next tested its FLS-targeting activity in vivo. We administered 2-month-old mice with rAAV9 or rAAV9.HAP-1 vectors via intra-articular injection. EGFP expression in the liver of mice treated with rAAV9.HAP-1 was comparatively lower than that in mice treated with rAAV9 (online supplemental figure S11A). Intriguingly, the fluorescent signal of EGFP in the joint from mice treated with rAAV9.HAP-1 was obviously stronger than that in rAAV9-treated mice (online supplemental figure S11A). The fluorescence microscopy images also confirmed that
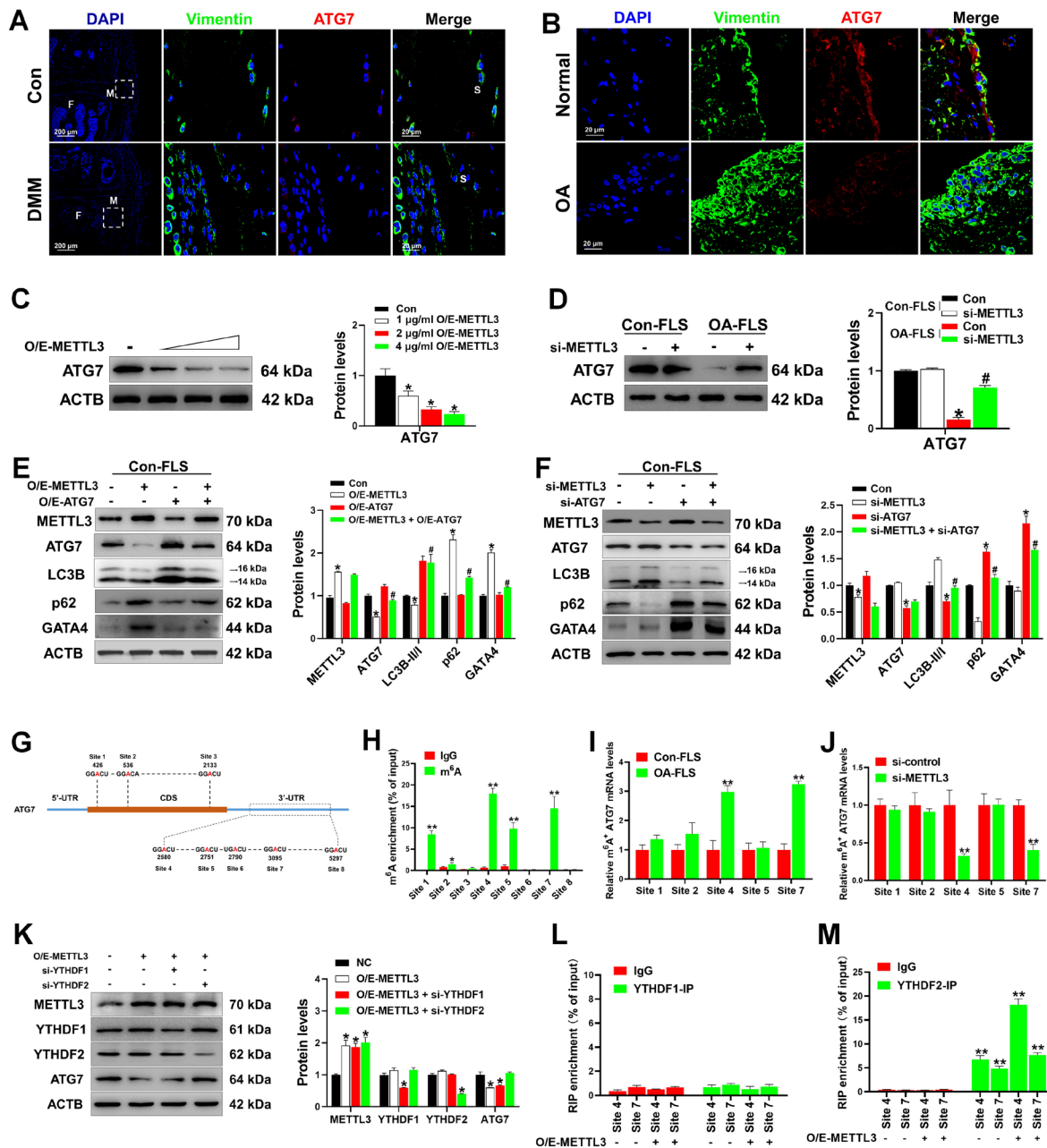
Figure 6 METTL3-mediated m⁶A modification induces the decay of the ATG7 transcript in YTHDF2-dependent manner. (A,B) The representative images of double immunofluorescent staining of vimentin and ATG7 in synovium from patients with OA (A) and post-traumatic mice (B) 8 weeks after DMM surgery. The dotted box indicates the amplified synovium regions. (C) Western blot analysis of protein level for ATG7 in human FLS (passage 2) after transfected with pcDNA3.1-METTL3 vector (O/E-METTL3,O/E) at different concentrations (1, 2 and 4 µg/mL) for 3 days. n=3. *P<0.05. (D) Western blot analysis of protein level for ATG7 in human Con-FLS and OA-FLS (passage 2) after transfected with si-METTL3) for 3 days. n=3. *P<0.05 vs Con-FLS; #P<0.05 vs OA-FLS. (E) Western blot analysis of protein levels for indicated genes (METTL3, ATG7, LC3B, p62 and GATA4) in human Con-FLS (passage 2) after transfection with or without O/E-METTL3 followed by treatment with or without pcDNA3.1-ATG7 vector (O/E-ATG7). n=3. *P<0.05 vs Con; #P<0.05 vs O/E-METTL3. (F) Western blot analysis of protein levels for indicated genes (METTL3, ATG7, LC3B, p62 and GATA4) in human Co-FLS (passage 2) after transfection with or without si-METTL3 followed by treatment with or without siRNA targeting ATG7 (si-ATG7). n=3. *P<0.05 vs Con; #P<0.05 vs si-ATG7. (G) Schematic diagram showing the position of m⁶A motifs within ATG7 transcript sequence. (H) MeRIP-qPCR analysis of m⁶A levels of ATG7 at different sites in human Con-FLS (passage 2). n=3. **P<0.01. (I) MeRIP-qPCR analysis of m⁶A levels of ATG7 in human FLS and OA-FLS. n=3. **P<0.01. (J) MeRIP-qPCR analysis of m⁶A levels of ATG7 in human FLS (passage 2) after transfection with or without si-METTL3. n=3. **P<0.01. (K) Western blot analysis of protein levels for METTL3, YTHDF1, YTHDF2 and ATG7 in human Con-FLS (passage 2) after transfection with or without O/E-METTL3, followed by treatment with or without siRNA targeting YTHDF1 or YTHDF2. n=3. *P<0.05. (O,P) RIP-qPCR analysis of the interaction of ATG7 with YTHDF1 (O) or YTHDF2 (P) in human Con-FLS (passage 2) transfected with or without O/E-METTL3. n=3. **P<0.01. All data were presented as the means±SEM. One-way analysis of variance with Dunnett's multiple comparisons (D–F,K–M) and paired t test (H, I,J) was used for statistical analysis. ATG7, autophagy-related 7; DMM, destabilisation of the medial meniscus; F, femur; FLS, fibroblast-like synoviocyte; M, meniscus; m⁶A, N6-methyladenosine; MeRIP, methylated RNA immunoprecipitation; METTLE3, methyltransferase-like 3; OA, osteoarthritis; O/E, overexpression; qPCR, quantitative PCR; RIP, RNA-immunoprecipitation; S, synovium; si-METTL3, siRNA targeting METTL3; siRNA, small interfering RNA; YTHDF, YTH N6-methyladenosine RNA-binding protein.
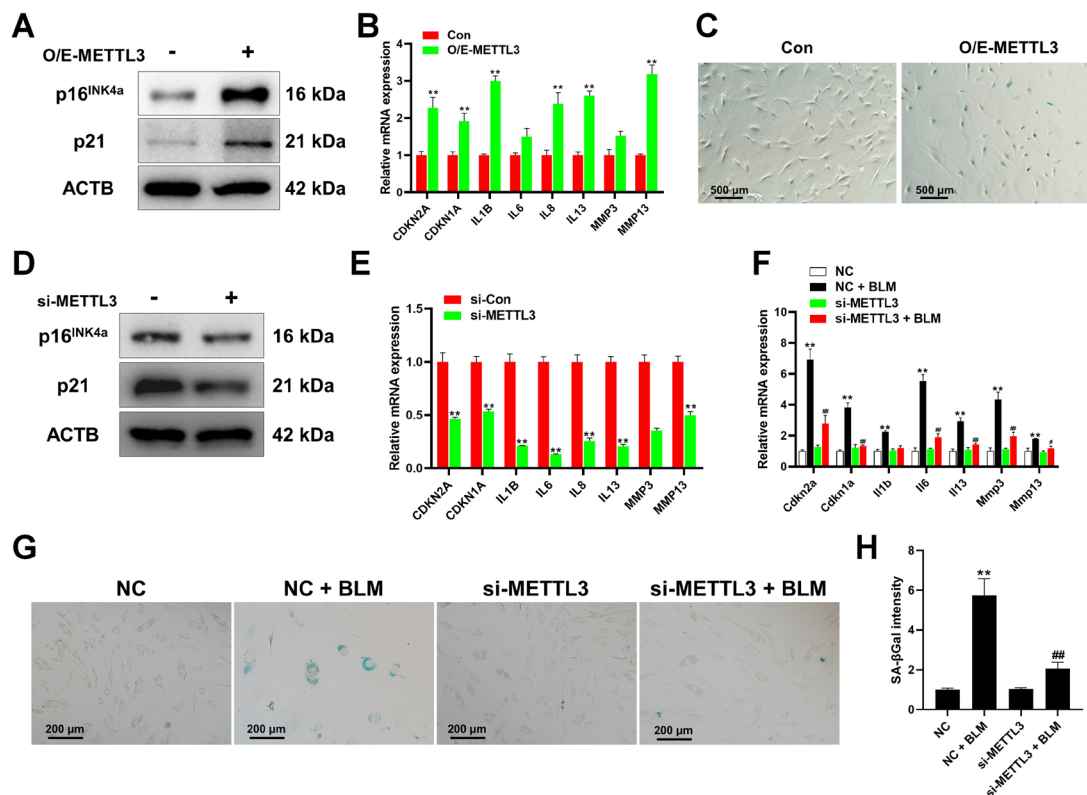
Figure 7 METTL3 regulates cellular senescence and SASP expression in FLS in vitro. (A) Western blot analysis of protein levels for p16^{INK4a} and p21 in human Con-FLS (passage 2) after transfection with or without pcDNA3.1-METTL3 vector (O/E-METTL3, O/E). (B) Q-PCR analysis of mRNA levels for SASP-related genes (CDKN2A, CDKN1A, IL-1β, IL-6, IL-13, MMP3 and MMP13) in human Con-FLS (passage 2) after transfected with or without O/E-METTL3. n=3, **p<0.01. (C) The representative images of SA-β-Gal staining for human Con-FLS (passage 2) transfected with or without O/E-METTL3. (D) Western blot analysis of protein levels for p16^{INK4a} and p21 in human OA-FLS (passage 2) after transfected with or without si-METTL3. (E) qPCR analysis of mRNA levels for SASP-related genes (CDKN2A, CDKN1A, IL-1β, IL-6, IL-13, MMP3 and MMP13) in human OA-FLS (passage 2) after transfection with or without si-METTL3. n=3. **P<0.01. (F) qPCR analysis of mRNA levels for SASP-related genes (Cdkn2a, Cdkn1a, IL-1β, IL-6, IL-13, MMP3 and MMP13) in mouse FLS (passage 2) after treatment with or without BLM (10 μM), accompanied with or without the transfection of si-METTL3. n=3. **P<0.01 vs NC, #P<0.05, ##P<0.01 vs NC +BLM. (G,H) The representative images of SA-β-Gal staining (G) and subsequent quantification of SA-β-Gal intensity (H) for mouse FLS (passage 2) after indicated treatment as in (F). n=3. **P<0.01 vs NC; #P<0.05, ##P<0.01 vs NC +BLM. All data were presented as the means±SEM. Paired t-test (B,E) and one-way analysis of variance with Dunnett's multiple comparisons (F,H) were used for statistical analysis. BLM, bleomycin; FLS, fibroblast-like synoviocyte; IL, interleukin; METTL3, methyltransferase-like 3; MMP, matrix metalloproteinase; mRNA, messenger RNA; OA, osteoarthritis; O/E, overexpression; qPCR, quantitative PCR; SA-β-Gal, senescence-associated β-galactosidase; SASP, enescence-associated secretory phenotype.

there were more EGFP-positive cells in the synovium of mice injected intra-articularly with rAAV9.HAP-1 than in mice treated with rAAV9, which were costained with vimentin (figure 8C and online supplemental figure S11B). These results demonstrate that the engineered VP2 capsid protein fused with HAP-1 improved the FLS tropism of rAAV9. In addition, as compared with chondrocytes or cartilage, the expression of METTL3 was significantly decreased in the FLSs and synovial tissues of mice treated with AAV9.HAP-1-si-METTL3, indicating that AAV9. HAP-1-si-METTL3 could specifically decrease the expression of METTL3 in FLS (online supplemental figure S12A,B).

We next examined whether intra-articular injection of AAV9. HAP-1-si-METTL3 could exert therapeutic effects in a DMM-induced OA mouse model. The results showed that the progressive cartilage degradation in DMM mice during OA development was significantly reversed after intra-articular injection of AAV9. HAP-1-si-METTL3 (figure 8D,E). In addition, we found that the levels of METTL3 and p16^{INK4a} in the synovium of mice treated with AAV9.HAP-1-si-METTL3 were markedly reduced, relative to those in mice treated with AAV9.HAP-1-NC (figure 8F and online supplemental figure S12C). Taken together, these results

demonstrate that delivery of si-METTL3 by the synovium-tropic AAV9.HAP-1 capsid could counteract OA progression in DMM-induced OA mouse models.

DISCUSSION

To date, ageing has always been considered an essential aetiological agent for OA, which is characterised by cellular senescence and progressive loss of tissue and organ function over time.[3 33] It has been demonstrated that local clearance of senescent cells could attenuate the progression of OA and create a proregenerative environment.[6] However, the molecular mechanisms underlying the relationship between ageing and OA pathogenesis remain unclear. In this study, we found extensive numbers of senescent FLSs in the progression of OA, which could promote cartilage dysfunction in vitro and in vivo (figures 1 and 2), indicating the critical role of senescent FLSs in OA pathogenesis. Thus, uncovering the mechanism of FLS senescence may provide new key targets for the clinical treatment of OA.

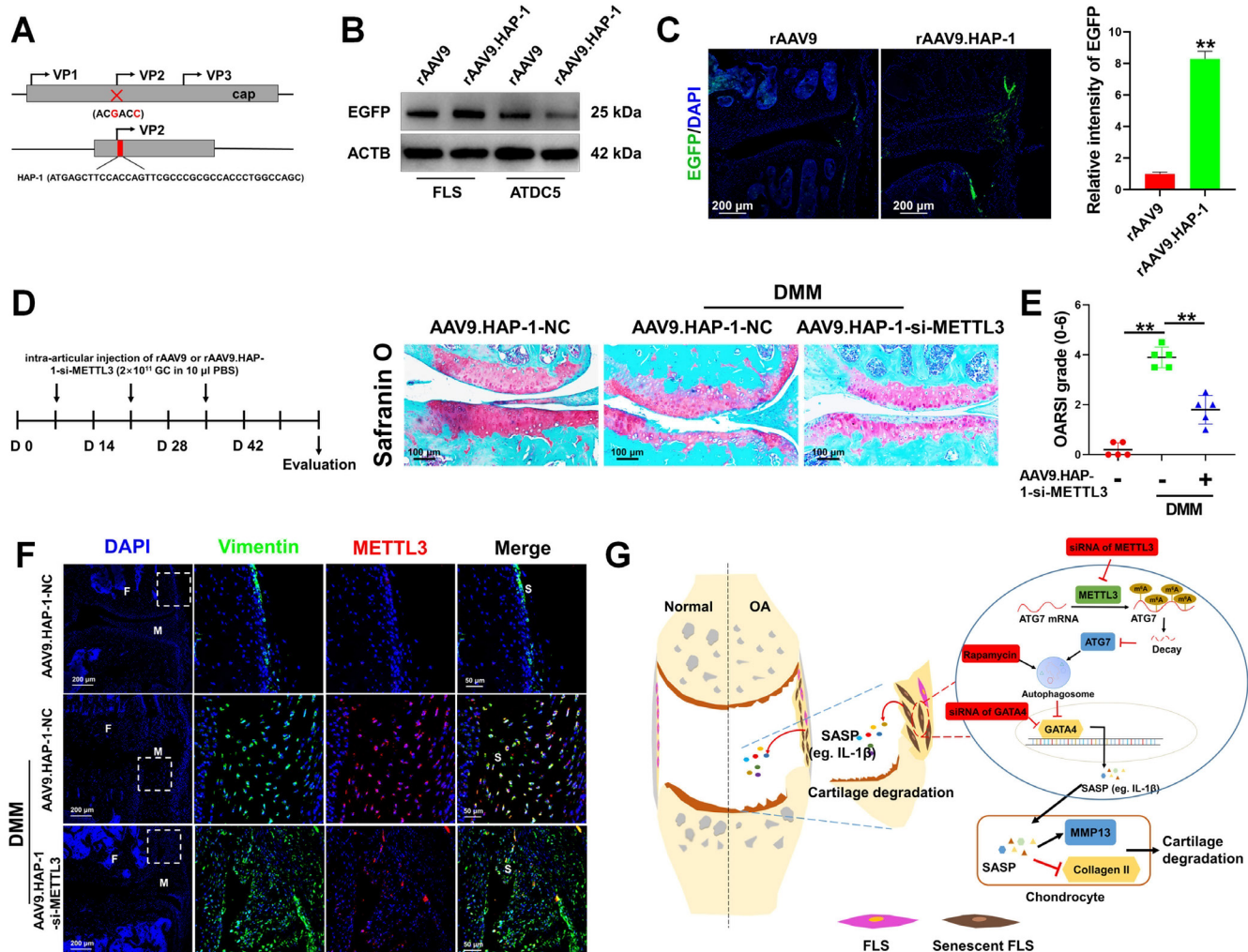It has been reported that OA deregulates common molecular and cellular mechanisms in chronic age-related diseases.[34]

Figure 8 Synovium-targeted inhibition of METTL3 alleviates the pathological progression of DMM-induced OA. (A) Diagram of construct for rationally designed synovium-specific AAV capsids. The synovium-targeting peptide motif (HAP-1, red) was inserted into the AAV9 capsid at the N-terminus of AAV9-VP2. (B) Western blot analysis of EGFP expression level in FLS (passage 2) and ATDC5 cells infected with rAAV9 or rAAV9.HAP-1 at the concentration of 10^{11} GC/mL. (C) Confocal microscope analysis of the EGFP expression in the knee joints from mice after intra-articular injection with rAAV9 or rAAV9.HAP-1. n=3. **P<0.01. (D) The diagram for experimental design (left) and the representative photomicrographs of Safranin-O/fast green staining for knee joint sections from DMM mice after intra-articular injection with rAAV9.HAP-1-NC and rAAV9.HAP-1-si-METTL3, respectively. (E) The severity of OA-like phenotype was analysed by grading histological sections in medial femoral condyles and the medial tibial plateau using the OARSI score system. n=4 of each group. **P<0.01. (F) The representative images of double immunofluorescent staining of vimentin and METTL3 in the knee joint from DMM mice after intra-articular injection with rAAV9.HAP-1-NC or rAAV9.HAP-1-si-METTL3. (G) Schematic representation of mechanisms by which FLS senescence mediates OA development. All data were presented as the means±SEM. Paired t-test (C) and one-way analysis of variance with Dunnett's multiple comparisons (E) was used for statistical analysis. DMM, destabilisation of the medial meniscus; EGFP, enhanced green fluorescent protein; F, femur; FLS, fibroblast-like synoviocyte; IL, interleukin; M, meniscus; METTL3, methyltransferase-like 3; OA, osteoarthritis; OARSI, Osteoarthritis Research Society International; S, synovium; SASP, senescence-associated secretory phenotype.

A common feature of these diseases is low-grade chronic systemic inflammation.[4 35] Emerging evidence demonstrated that increased production of proinflammatory and matrix-degrading molecules, also known as SASP, could be an important mechanism in OA, leading to a chronically inflamed microenvironment and complicating the implantation of stem cells to repair the joint injury.[36] Autophagy is a cellular homeostasis mechanism for the removal of dysfunctional organelles and macromolecules. Defective autophagy is involved in the pathogenesis of age-related diseases and promotes inflammation in multiple tissues.[37 38] During ageing, autophagy gradually decreases and induces senescence, which ultimately result in increased OA severity.[14] Augmentation of homeostasis mechanisms is discussed

as a novel avenue to delay joint ageing and reduce OA risk. In our study, we found impaired autophagy in the OA synovium, and activation of autophagy effectively suppressed cellular senescence in FLSs. In addition, we found that GATA4, a novel senescence regulator,[8] was significantly elevated in OA-FLS. Upregulation of GATA4 dramatically induced the expression of SASP and markers of cellular senescence, and autophagy regulated FLS senescence in a GATA4-dependent manner. Our data suggest that autophagy regulates FLS senescence, and that modification of autophagy may provide a potential strategy for OA intervention.

Recent studies have shown that m⁶A modification is widespread throughout the transcriptome, accounting for over 80%

of all RNA methylation modifications.[39] As one of the most common RNA modifications, m6A modification plays critical roles in various physiological processes, including tumour invasion, cellular senescence and cell differentiation.[40–42] It has been reported that m6A-modified mRNA transcripts are less stable due to YTHDF2-mediated mRNA decay,[31] and that the binding sites of YTHDF2 were usually enriched around stop codons and in 3′UTRs of mRNA.[22] In our study, we observed enhanced m6A modification in OA-FLS, accompanied by increased expression of METTL3. Accumulating evidence has confirmed that increased METTL3 may result in enhanced m6A levels,[43] and that elevated METTL3 could suppress autophagic flux by methylating the mRNA of transcription factor EB.[28] In senescent FLSs, we identified ATG7, which is required for the elongation of phagophores during autophagosome formation[30 44] and plays a key role in METTL3-mediated autophagy suppression. In addition, we demonstrated that METTL3-mediated m6A modification of ATG7 is further regulated by YTHDF2. Using RIP-qPCR analysis, we validated the stronger YTHDF2 enrichment at ATG7 transcripts, demonstrating that ATG7 was the target gene of YTHDF2, but not YTHDF1. In vitro, loss of METTL3 in OA-FLS recovered autophagy and decreased the expression of GATA4. Targeted inhibition of METTL3 in the synovium via local intra-articular administration of rAAV9.HAP-1-si-METTL3 effectively decreased the number of senescent cells in the synovium and inhibited articular cartilage erosion.

In summary, the findings presented here expand our knowledge on the mechanisms, by which METTL3 plays a fundamental role in promoting cellular senescence and OA progression. METTL3 carries out these functions by regulating autophagy and affecting the stability of the ATG7 transcript in an m6A-YTHDF2-dependent manner (figure 8G). Our study highlights the functional importance of the m6A methylation machinery in autophagy, which provides insights into the underlying molecular mechanisms of METTL3 in regulating cellular senescence and the development of therapeutic strategies for the treatment of OA.

ORCID iDs
Qing Jiang http://orcid.org/0000-0002-2552-9686
Baosheng Guo http://orcid.org/0000-0002-4510-5418

REFERENCES

1 Glyn-Jones S, Palmer AJR, Agricola R, et al. Osteoarthritis. Lancet 2015;386:376–87.
2 Losina E, Weinstein AM, Reichmann WM, et al. Lifetime risk and age at diagnosis of symptomatic knee osteoarthritis in the US. Arthritis Care Res 2013;65:703–11.
3 Lotz M, Loeser RF. Effects of aging on articular cartilage homeostasis. Bone 2012;51:241–8.
4 Mobasheri A, Matta C, Zákány R, et al. Chondrosenescence: definition, hallmarks and potential role in the pathogenesis of osteoarthritis. Maturitas 2015;80:237–44.
5 Wolfenson H, Yang B, Sheetz MP. Steps in mechanotransduction pathways that control cell morphology. Annu Rev Physiol 2019;81:585–605.
6 Jeon OH, Kim C, Laberge R-M, et al. Local clearance of senescent cells attenuates the development of post-traumatic osteoarthritis and creates a pro-regenerative environment. Nat Med 2017;23:775–81.
7 Attur MG, Patel IR, Patel RN, et al. Autocrine production of IL-1 beta by human osteoarthritis-affected cartilage and differential regulation of endogenous nitric oxide, IL-6, prostaglandin E2, and IL-8. Proc Assoc Am Physicians 1998;110:65–72.
8 Kang C, Xu Q, Martin TD, et al. The DNA damage response induces inflammation and senescence by inhibiting autophagy of GATA4. Science 2015;349:aaa5612.
9 Caramés B, Hasegawa A, Taniguchi N, et al. Autophagy activation by rapamycin reduces severity of experimental osteoarthritis. Ann Rheum Dis 2012;71:575–81.
10 Ballabio A, Bonifacino JS. Lysosomes as dynamic regulators of cell and organismal homeostasis. Nat Rev Mol Cell Biol 2020;21:101–18.
11 Stead ER, Castillo-Quan JI, Miguel VEM, et al. Agephagy - adapting autophagy for health during aging. Front Cell Dev Biol 2019;7:308.
12 Ge Y, Zhou S, Li Y, et al. Estrogen prevents articular cartilage destruction in a mouse model of AMPK deficiency via ERK-mTOR pathway. Ann Transl Med 2019;7:336.
13 Terman A, Kurz T, Navratil M, et al. Mitochondrial turnover and aging of long-lived postmitotic cells: the mitochondrial-lysosomal axis theory of aging. Antioxid Redox Signal 2010;12:503–35.
14 Caramés B, Taniguchi N, Otsuki S, et al. Autophagy is a protective mechanism in normal cartilage, and its aging-related loss is linked with cell death and osteoarthritis. Arthritis Rheum 2010;62:791–801.
15 Padmanabhan K, Robles MS, Westerling T, et al. Feedback regulation of transcriptional termination by the mammalian circadian clock PERIOD complex. Science 2012;337:599–602.
16 Hussain S, Sajini AA, Blanco S, et al. NSun2-mediated cytosine-5 methylation of vault noncoding RNA determines its processing into regulatory small RNAs. Cell Rep 2013;4:255–61.
17 Meyer KD, Jaffrey SR. The dynamic epitranscriptome: N6-methyladenosine and gene expression control. Nat Rev Mol Cell Biol 2014;15:313–26.
18 Jin S, Zhang X, Miao Y, et al. m6A RNA modification controls autophagy through upregulating ULK1 protein abundance. Cell Res 2018;28:955–7.
19 Li Q, Li X, Tang H, et al. NSUN2-Mediated m5C methylation and METTL3/METTL14-Mediated m6A methylation cooperatively enhance p21 translation. J Cell Biochem 2017;118:2587–98.
20 Xiang Y, Laurent B, Hsu C-H, et al. RNA m6A methylation regulates the ultraviolet-induced DNA damage response. Nature 2017;543:573–6.
21 Liu J, Eckert MA, Harada BT, et al. m6A mRNA methylation regulates AKT activity to promote the proliferation and tumorigenicity of endometrial cancer. Nat Cell Biol 2018;20:1074–83.
22 Shi H, Wei J, He C. Where, when, and how: context-dependent functions of RNA methylation writers, readers, and erasers. Mol Cell 2019;74:640–50.
23 Shi W, Zheng Y, Luo S, et al. METTL3 promotes activation and inflammation of FLSs through the NF-κB signaling pathway in rheumatoid arthritis. Front Med 2021;8:607585.
24 Xiao L, Zhao Q, Hu B, et al. METTL3 promotes IL-1β-induced degeneration of endplate chondrocytes by driving m6A-dependent maturation of miR-126-5p. J Cell Mol Med 2020;24:14013–25.
25 Cuervo AM, Bergamini E, Brunk UT, et al. Autophagy and aging: the importance of maintaining "clean" cells. Autophagy 2005;1:131–40.
26 He C, Klionsky DJ. Regulation mechanisms and signaling pathways of autophagy. Annu Rev Genet 2009;43:67–93.
27 Zhu J, Dagda RK, Chu CT. Monitoring mitophagy in neuronal cell cultures. Methods Mol Biol 2011;793:325–39.
28 Song H, Feng X, Zhang H, et al. METTL3 and ALKBH5 oppositely regulate m6A modification of TFEB mRNA, which dictates the fate of hypoxia/reoxygenation-treated cardiomyocytes. Autophagy 2019;15:1419–37.

29 Schwartz S, Mumbach MR, Jovanovic M, *et al*. Perturbation of m6A writers reveals two distinct classes of mRNA methylation at internal and 5' sites. *Cell Rep* 2014;8:284–96.

30 Levine B, Kroemer G. Biological functions of autophagy genes: a disease perspective. *Cell* 2019;176:11–42.

31 Wang X, Lu Z, Gomez A, *et al*. N6-methyladenosine-dependent regulation of messenger RNA stability. *Nature* 2014;505:117–20.

32 Mi Z, Lu X, Mai JC, *et al*. Identification of a synovial fibroblast-specific protein transduction domain for delivery of apoptotic agents to hyperplastic synovium. *Mol Ther* 2003;8:295–305.

33 Flatt T. A new definition of aging? *Front Genet* 2012;3:148.

34 Childs BG, Durik M, Baker DJ, *et al*. Cellular senescence in aging and age-related disease: from mechanisms to therapy. *Nat Med* 2015;21:1424–35.

35 Greene MA, Loeser RF. Aging-Related inflammation in osteoarthritis. *Osteoarthritis Cartilage* 2015;23:1966–71.

36 Atesok K, Fu FH, Sekiya I, *et al*. Stem cells in degenerative orthopaedic pathologies: effects of aging on therapeutic potential. *Knee Surg Sports Traumatol Arthrosc* 2017;25:626–36.

37 Carneiro LAM, Travassos LH. The interplay between NLRs and autophagy in immunity and inflammation. *Front Immunol* 2013;4:361.

38 Lotz M, Caramés B. Autophagy: a new therapeutic target in cartilage injury and osteoarthritis. *J Am Acad Orthop Surg* 2012;20:261–2.

39 Zheng H-X, Zhang X-S, Sui N. Advances in the profiling of N^6-methyladenosine (m^{6}A) modifications. *Biotechnol Adv* 2020;45:107656.

40 He L, Li H, Wu A, *et al*. Functions of N6-methyladenosine and its role in cancer. *Mol Cancer* 2019;18:176.

41 Vu LP, Pickering BF, Cheng Y, *et al*. The N^6-methyladenosine (m^{6}A)-forming enzyme METTL3 controls myeloid differentiation of normal hematopoietic and leukemia cells. *Nat Med* 2017;23:1369–76.

42 Wu Z, Shi Y, Lu M, *et al*. METTL3 counteracts premature aging via m6A-dependent stabilization of MIS12 mRNA. *Nucleic Acids Res* 2020;48:11083–96.

43 Choe J, Lin S, Zhang W, *et al*. mRNA circularization by METTL3-eIF3h enhances translation and promotes oncogenesis. *Nature* 2018;561:556–60.

44 Wesselborg S, Stork B. Autophagy signal transduction by ATG proteins: from hierarchies to networks. *Cell Mol Life Sci* 2015;72:4721–57.